

Supporting Information

Physical and electrochemical properties of new structurally flexible imidazolium phosphate ionic liquids

Sourav Bhowmick^{1*}, Andrei Filippov¹, Inayat Ali Khan¹, and Faiz Ullah Shah^{1*}

¹Chemistry of Interfaces, Luleå University of Technology, SE-971 87 Luleå, Sweden

*Corresponding:

Email: sourav.bhowmick@associated.ltu.se

Email: faiz.ullah@ltu.se

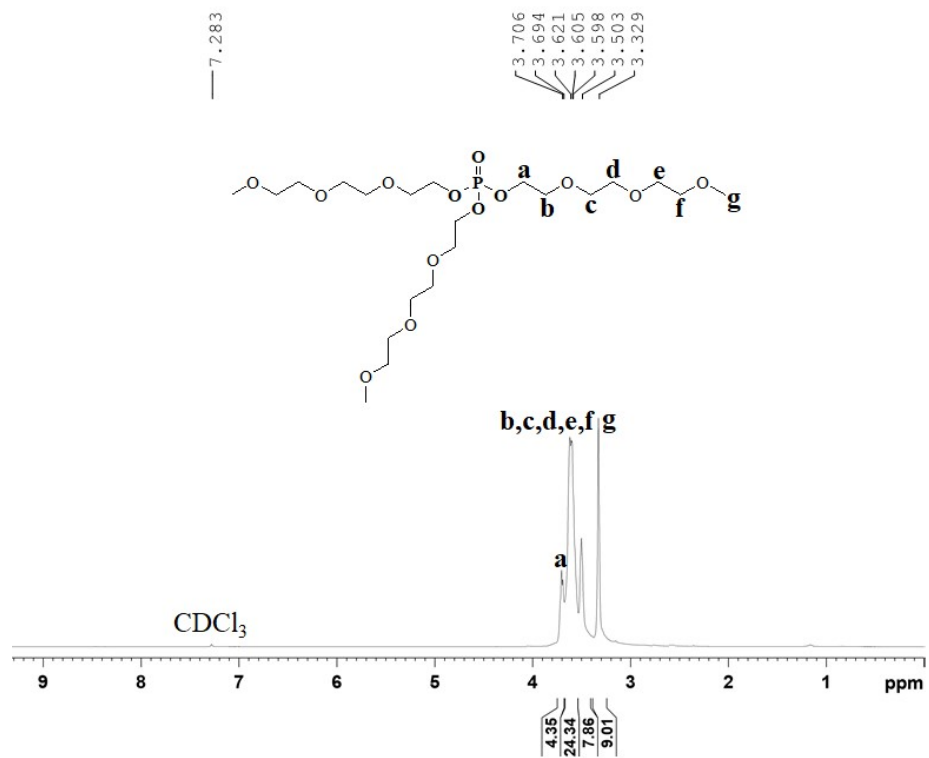


Figure S1: ¹H NMR spectrum of TMOP.

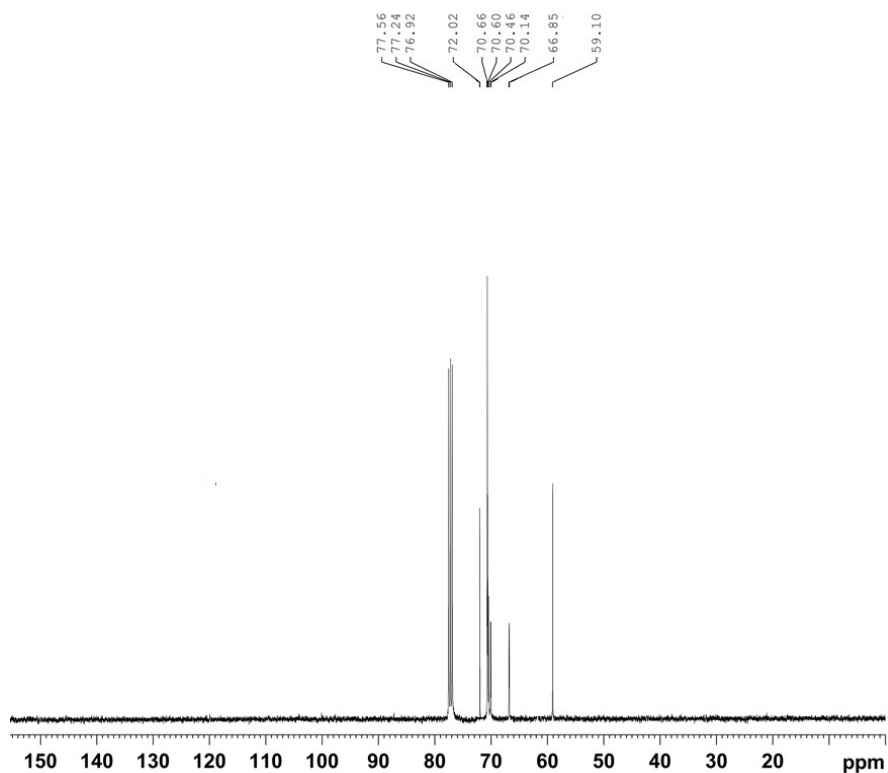


Figure S2: ¹³C NMR spectrum of TMOP.

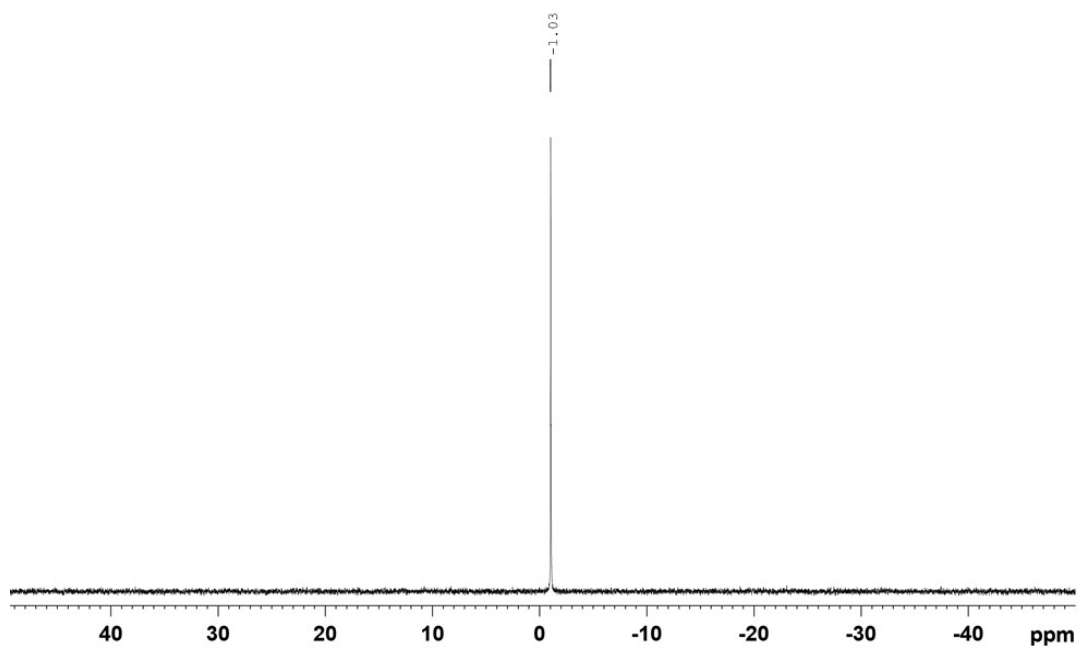


Figure S3: ³¹P NMR spectrum of TMOP.

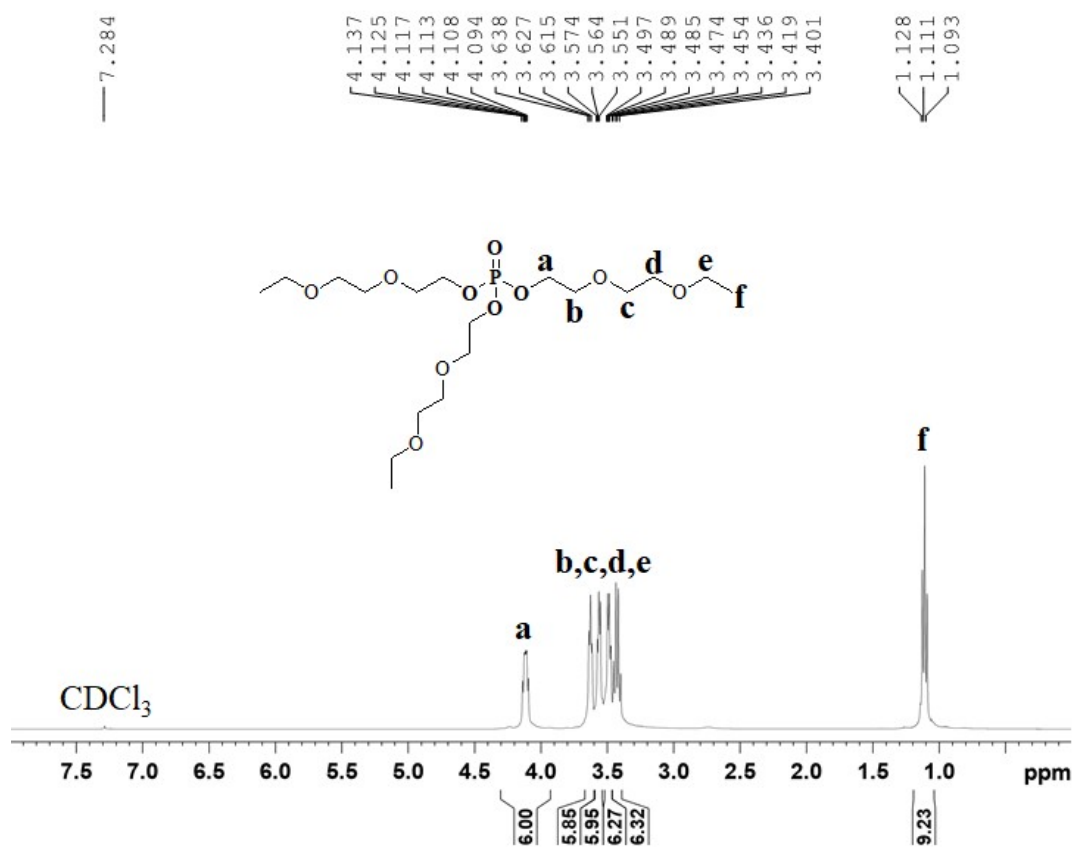


Figure S4: ¹H NMR spectrum of TEOP.

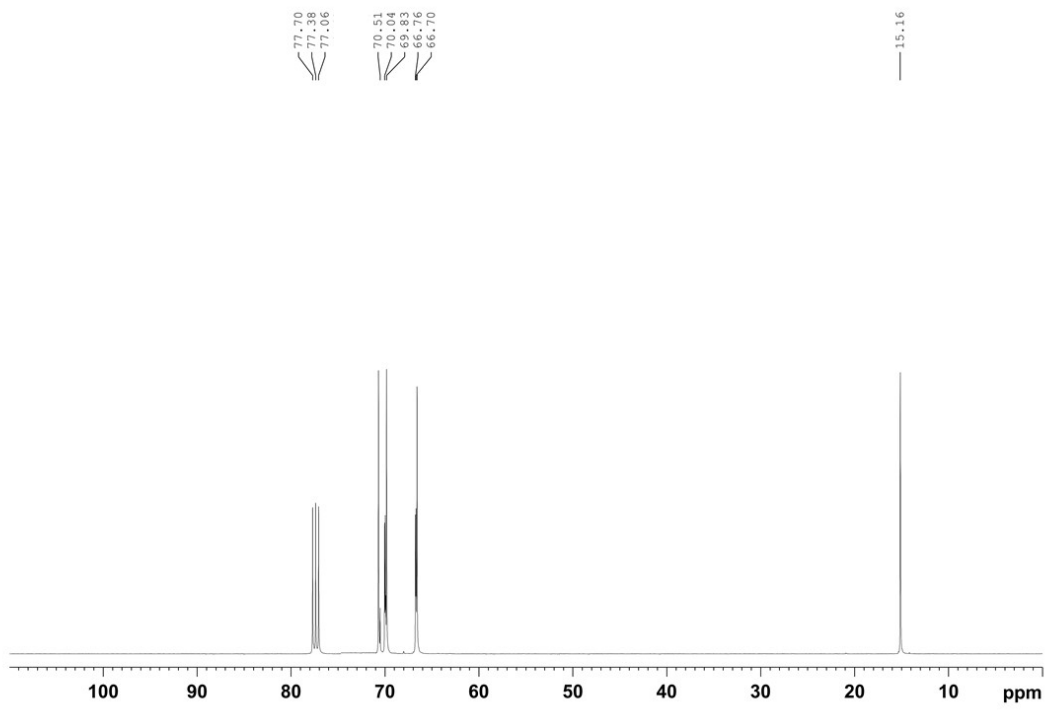


Figure S5: ¹³C NMR spectrum of TEOP.

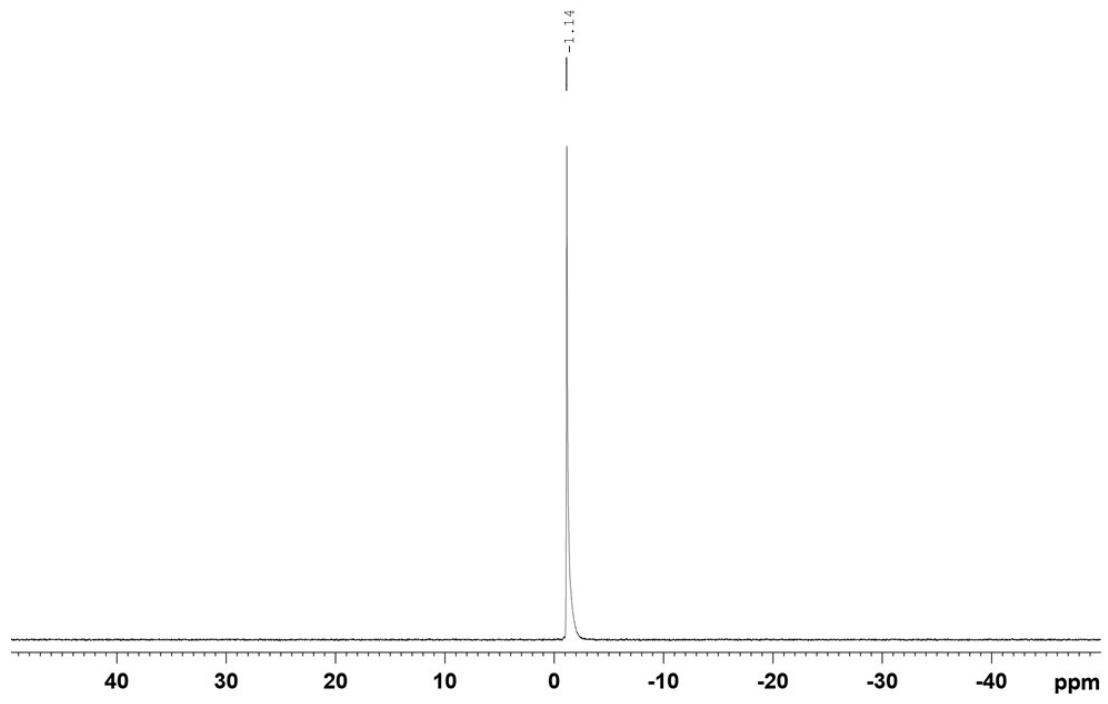


Figure S6: ³¹P NMR spectrum of TEOP.

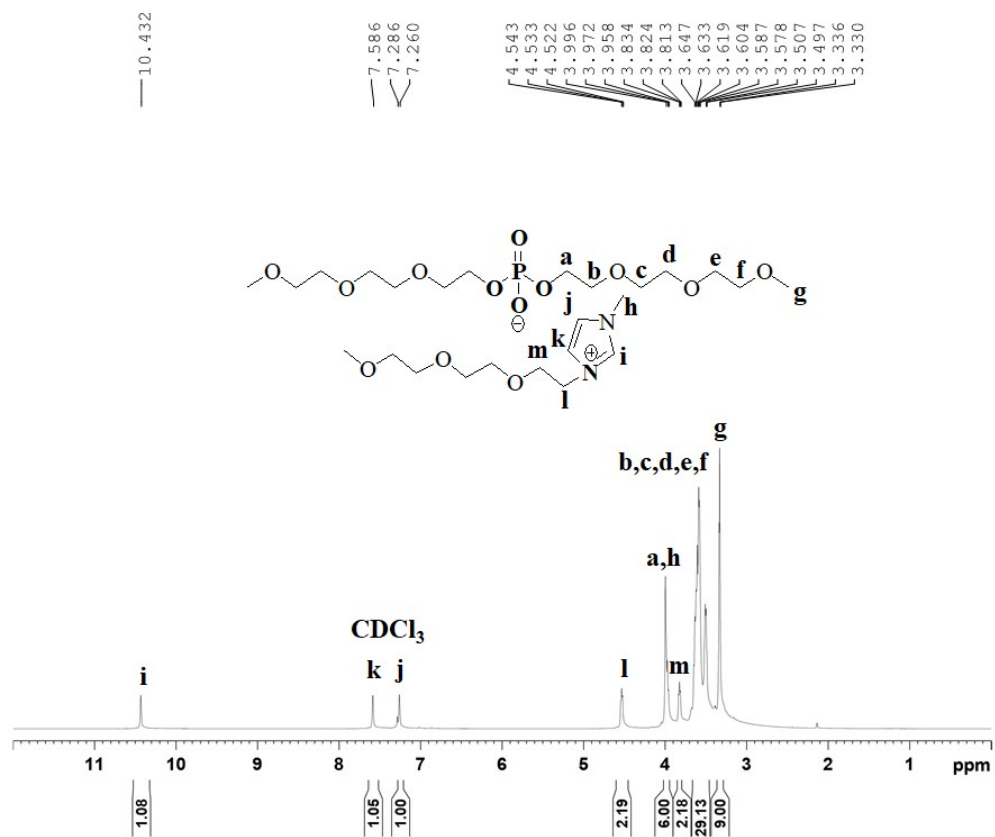


Figure S7: ^1H NMR spectrum of $[\text{MmMIm}][\text{TEEP}]$.

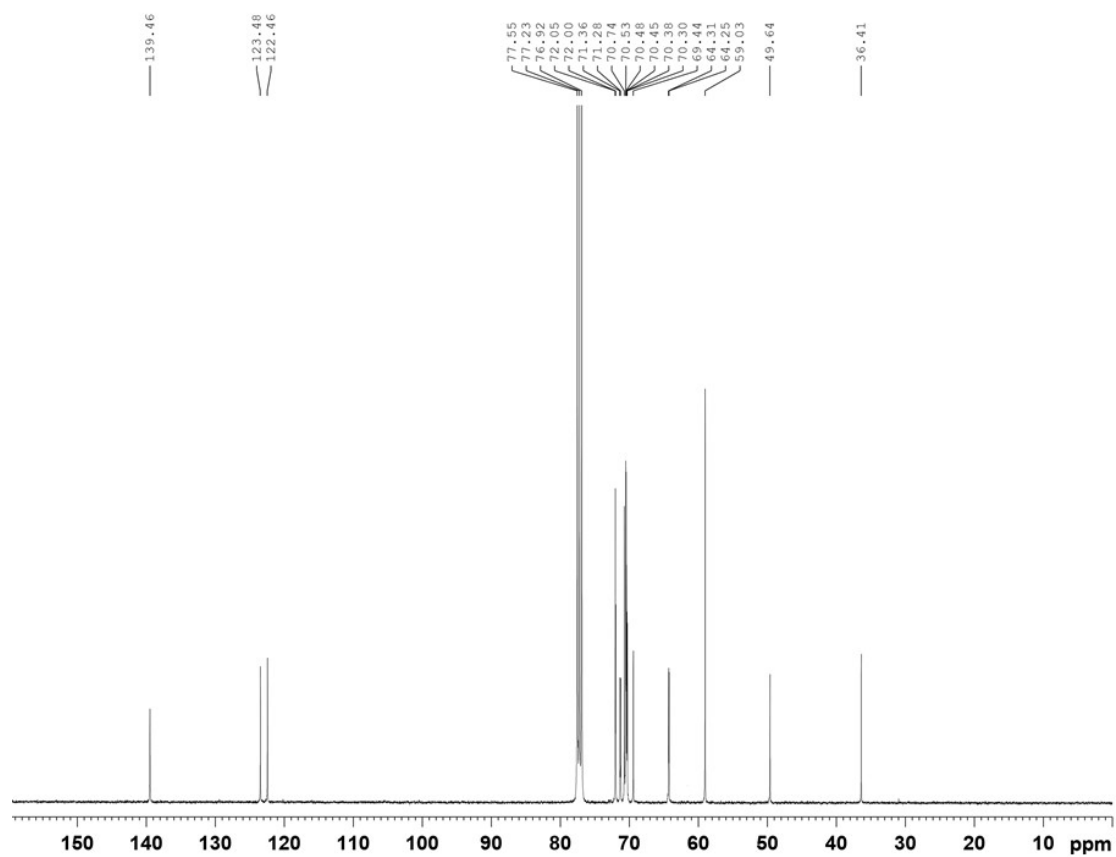


Figure S8: ^{13}C NMR spectrum of $[\text{MmMIm}][\text{TEEP}]$.

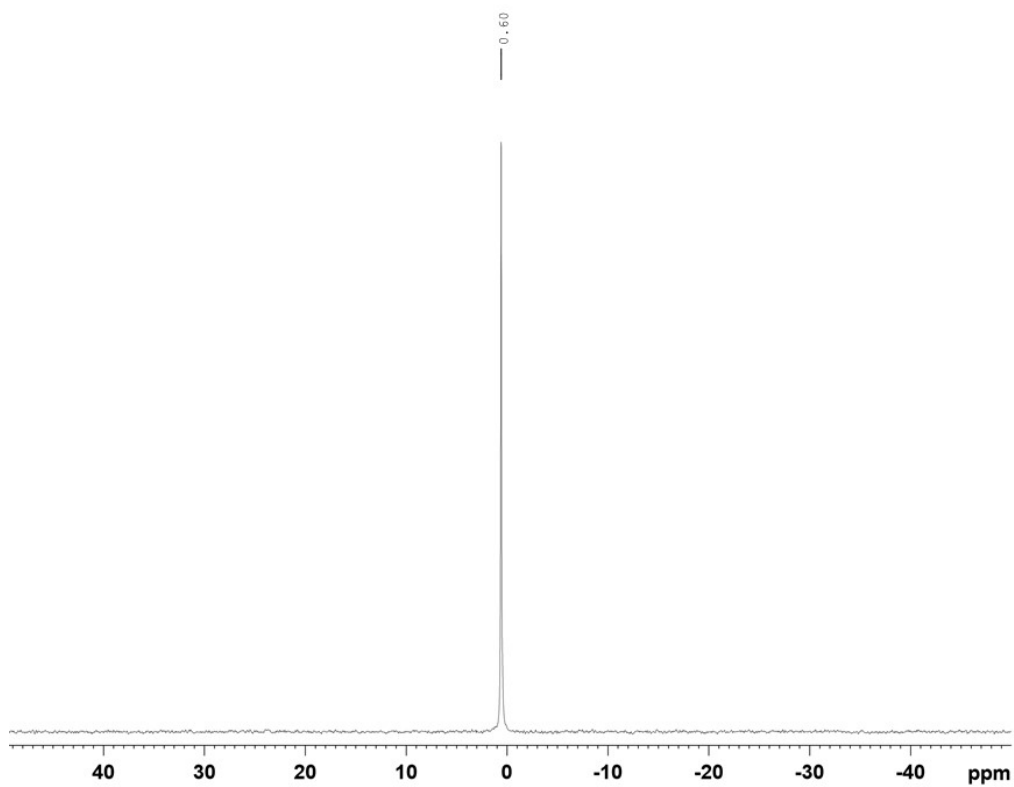


Figure S9: ^{31}P NMR spectrum of [MmMIm][TEEP].

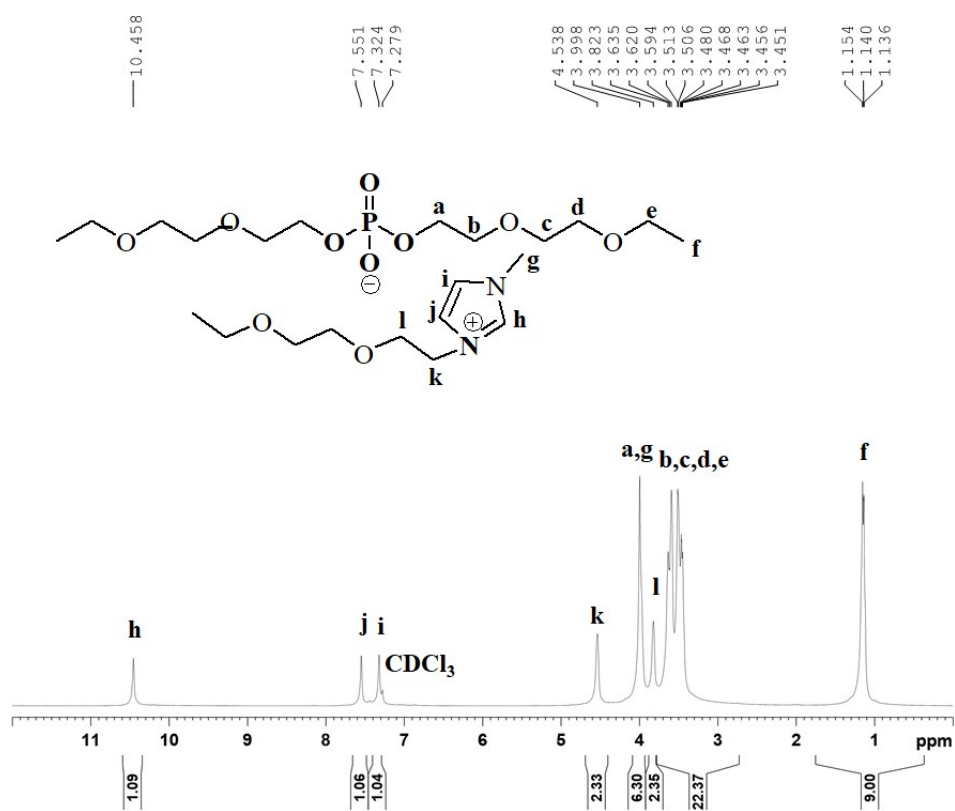


Figure S10: ^1H NMR spectrum of [EmMIm][DEEP].

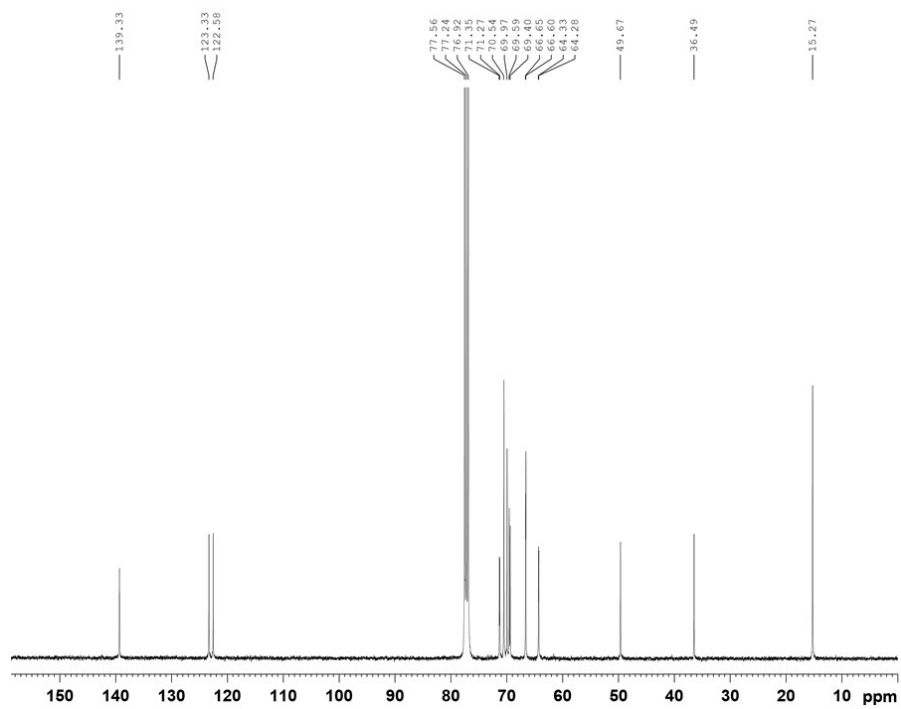


Figure S11: ¹³C NMR spectrum of [EmMIm][DEEP].

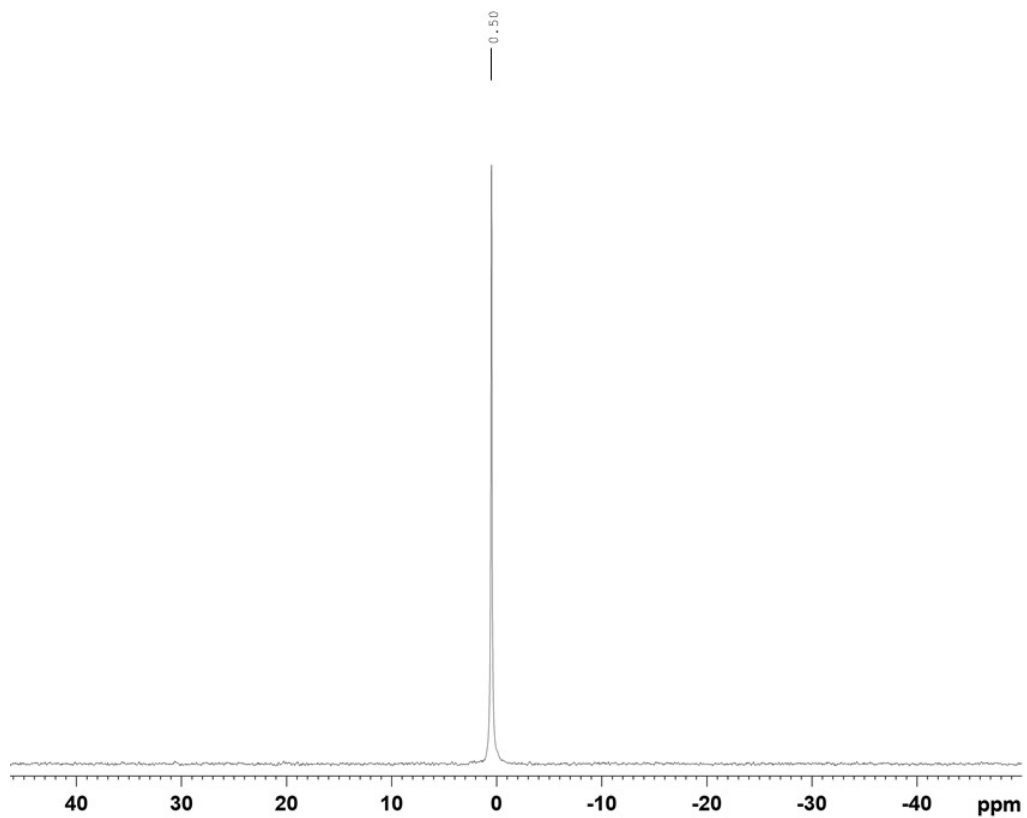


Figure S12: ³¹P NMR spectrum of [EmMIm][DEEP].

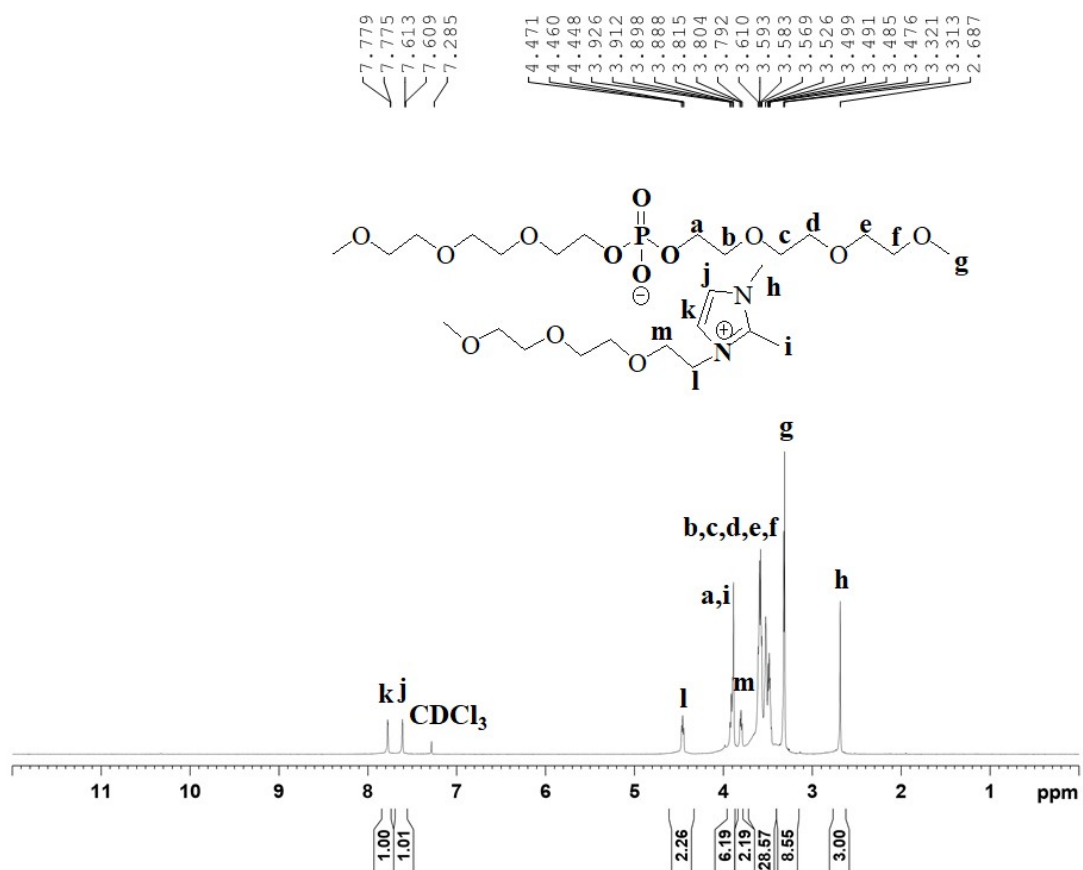


Figure S13: ¹H NMR spectrum of [MmDMIIm][TEEP].

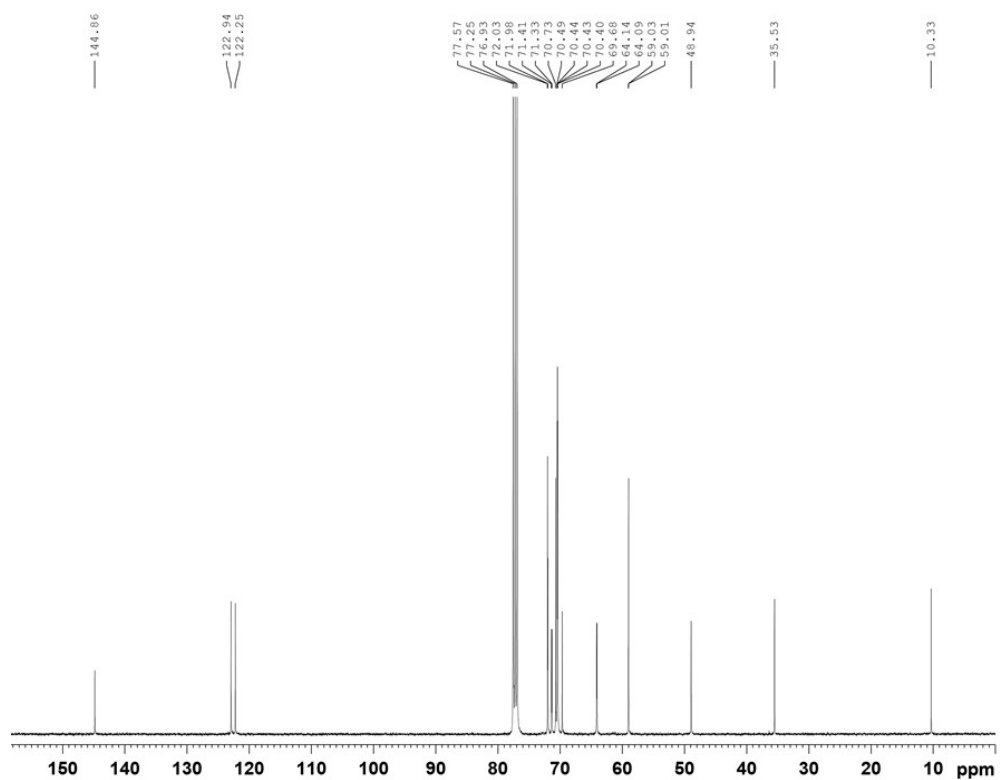


Figure S14: ¹³C NMR spectrum of [MmDMIIm][TEEP].

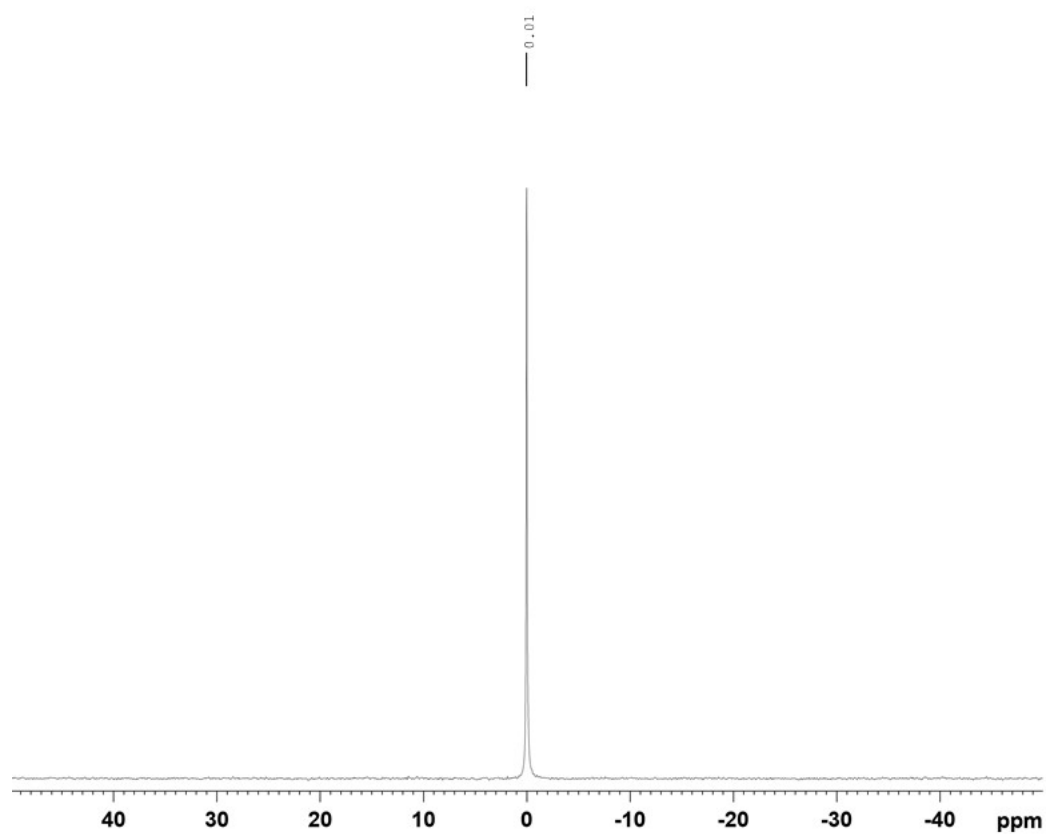


Figure S15: ^{31}P NMR spectrum of $[\text{MmDMIm}][\text{TEEP}]$.

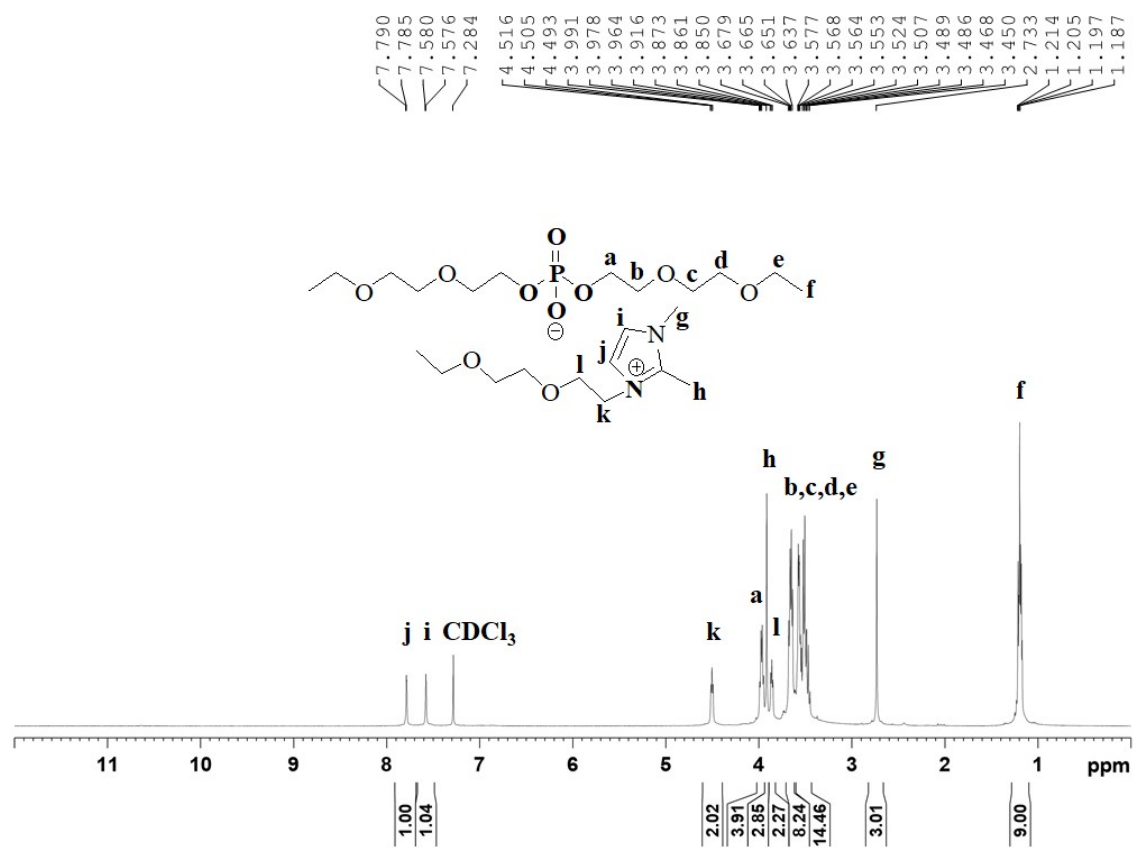


Figure S16: ^1H NMR spectrum of $[\text{EmDMIm}][\text{DEEP}]$.

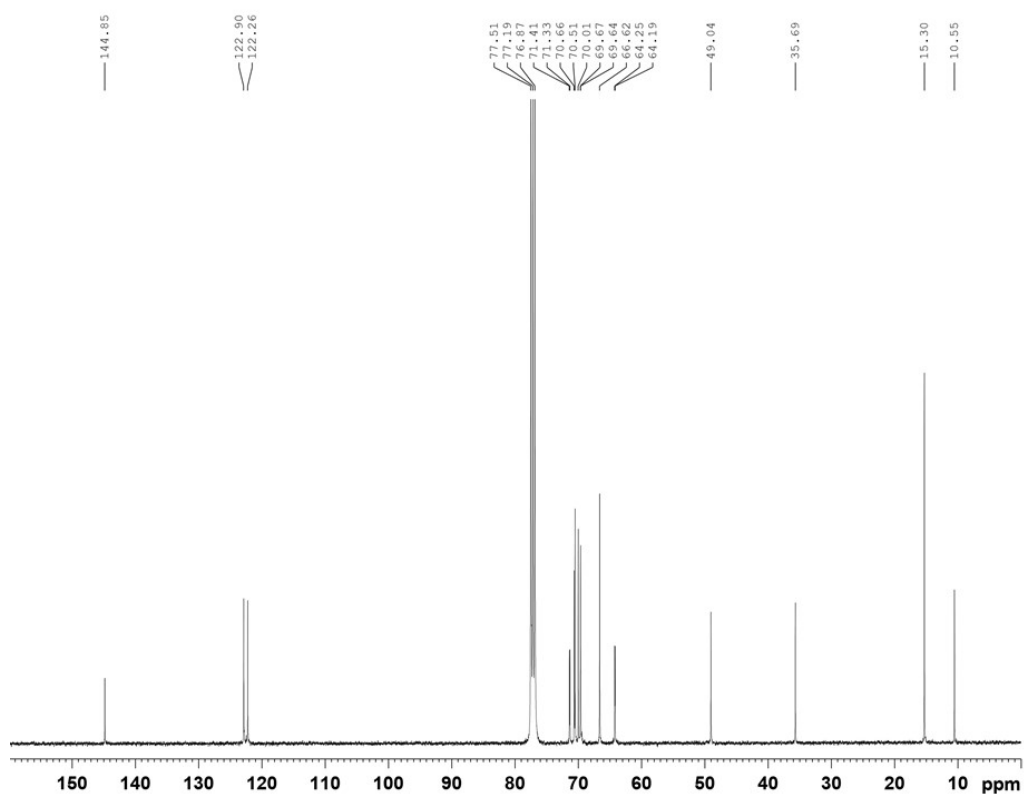


Figure S17: ^{13}C NMR spectrum of [EmDMIm][DEEP].

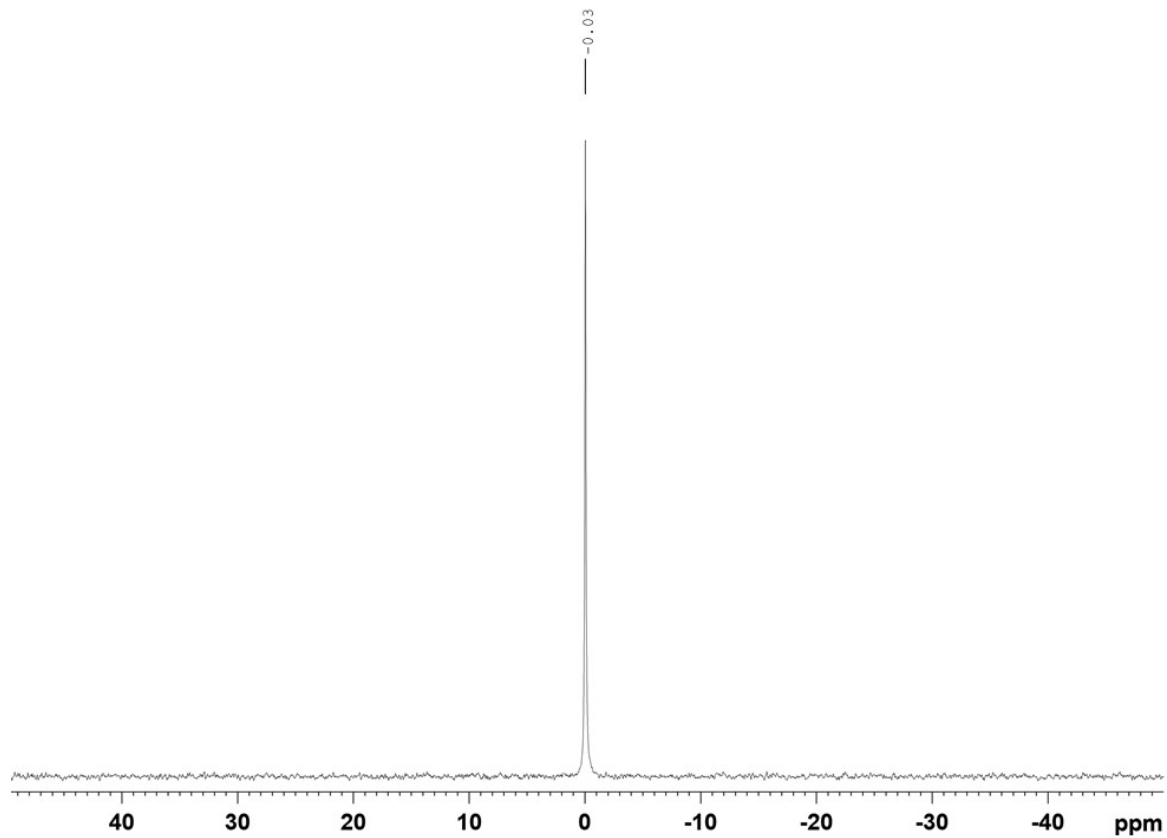


Figure S18: ^{31}P NMR spectrum of [EmDMIm][DEEP].

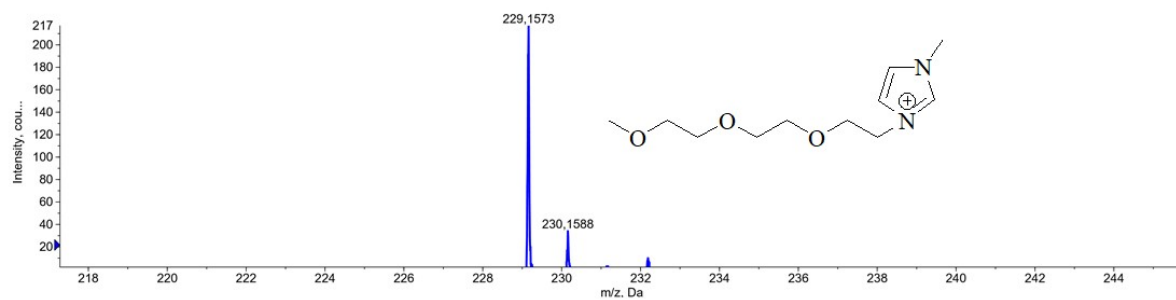
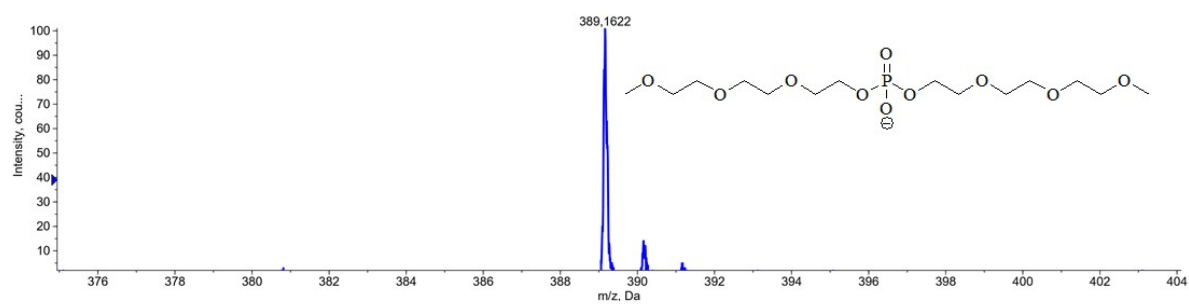


Figure S19. ESI-MS of [MmMIm][TEEP].

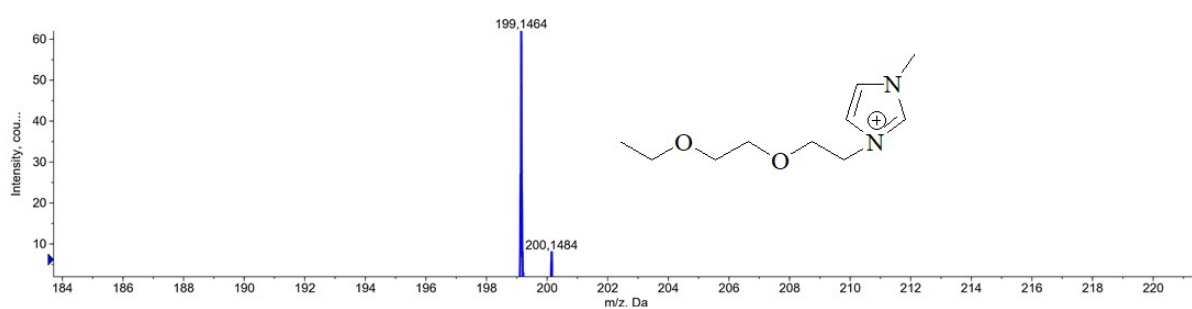
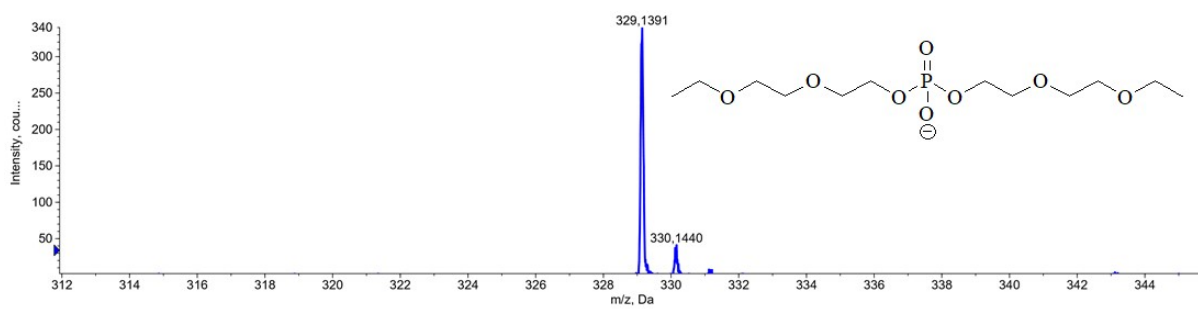


Figure S20. ESI-MS of [EmMIm][DEEP].

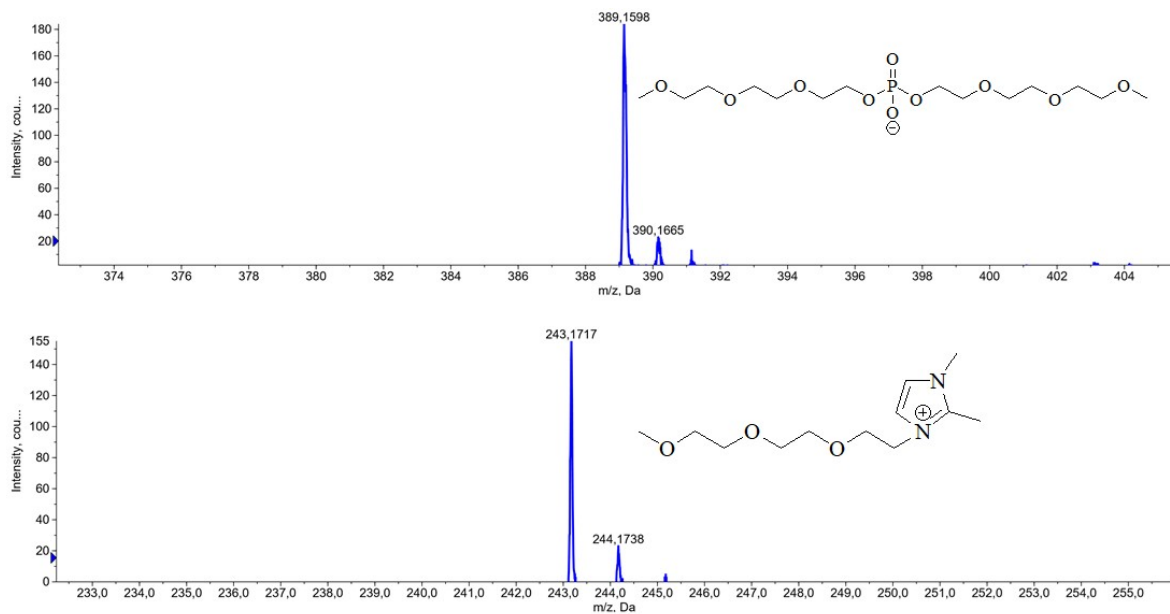


Figure S21. ESI-MS of [MmDMIm][TEEP].

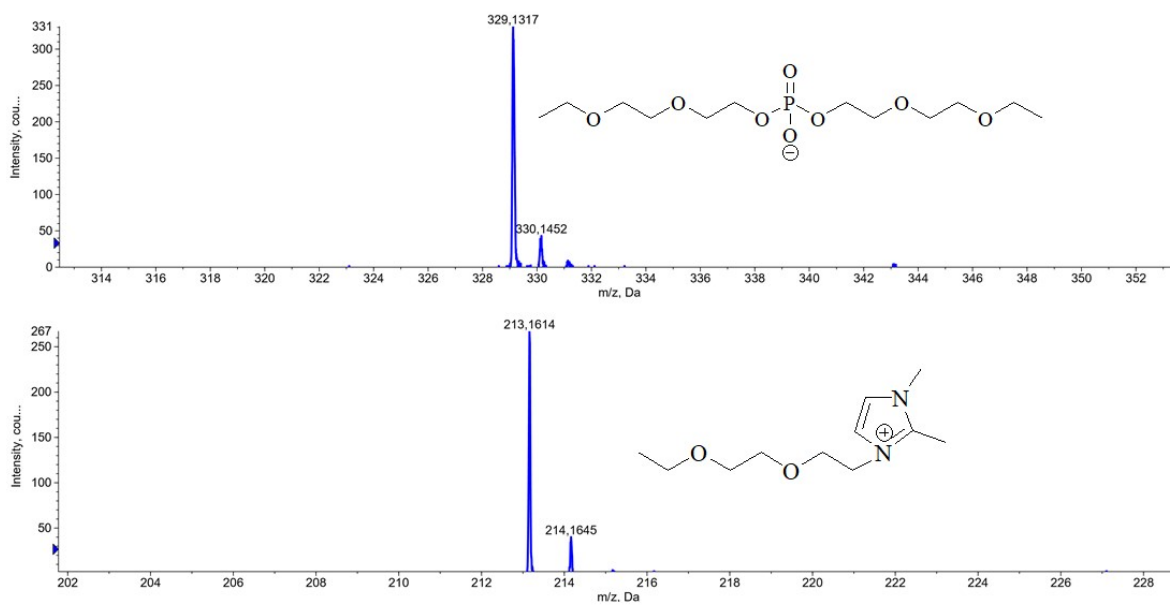


Figure S22. ESI-MS of [EmDMIm][DEEP].

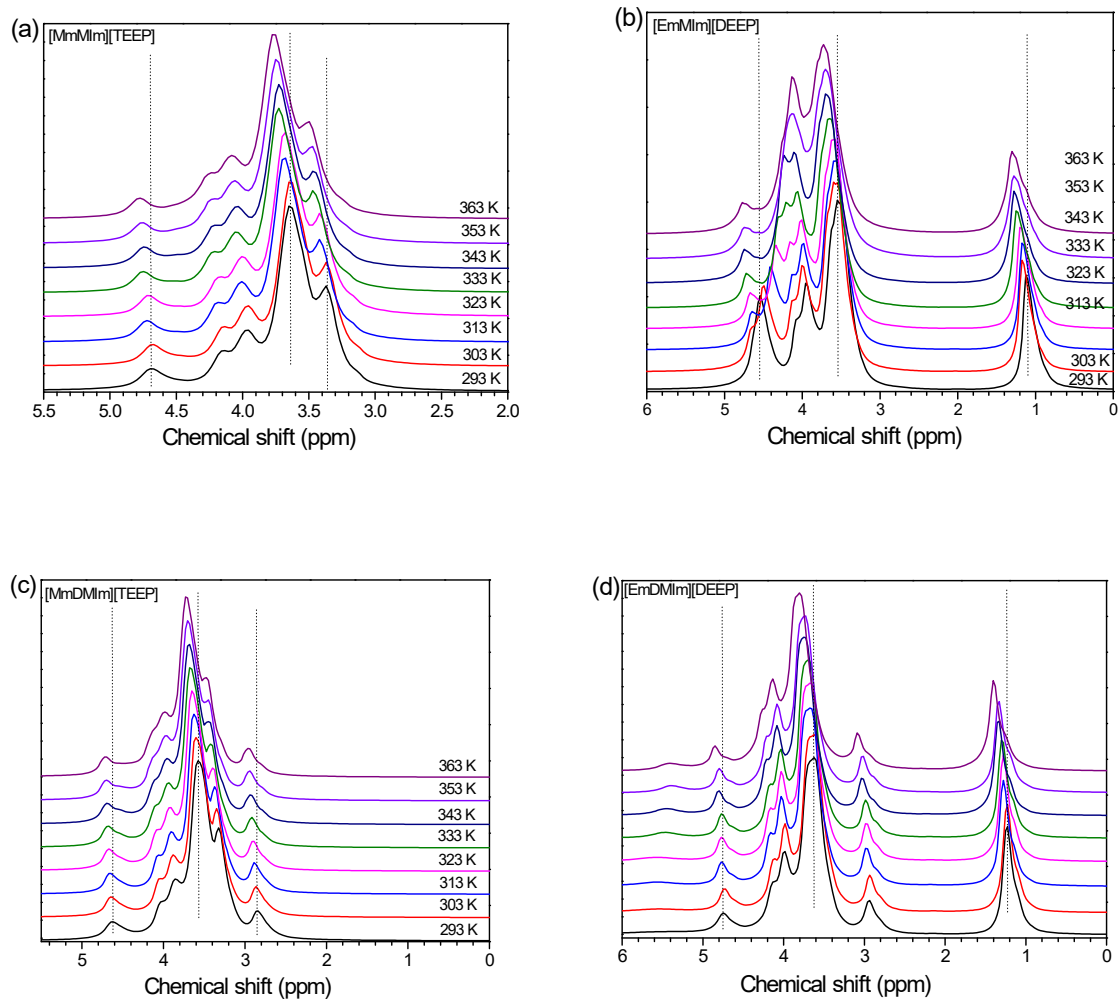


Figure S23. Variable temperature chemical shifts ^1H NMR spectra of four neat ILs.

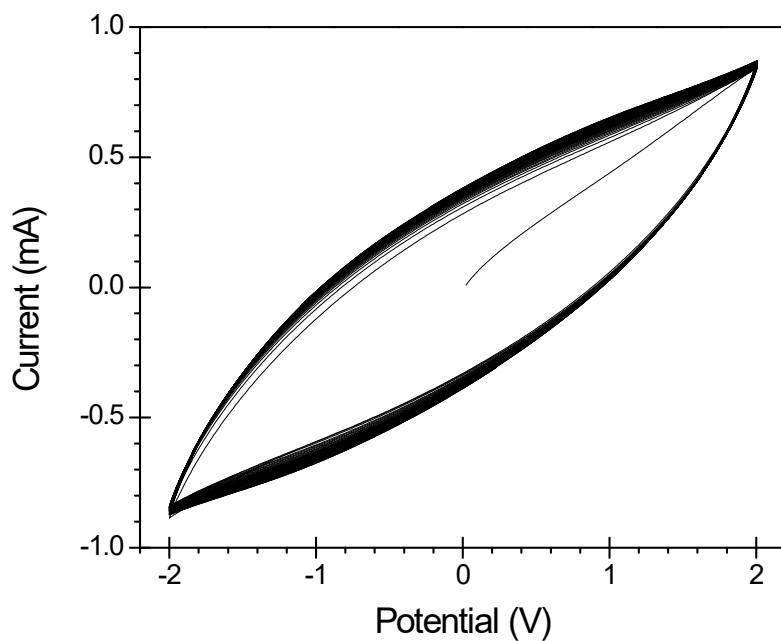


Figure S24. CV cycles (60) at 0.005 V s^{-1} and at $20 \text{ }^\circ\text{C}$ for the activation of supercapacitor.

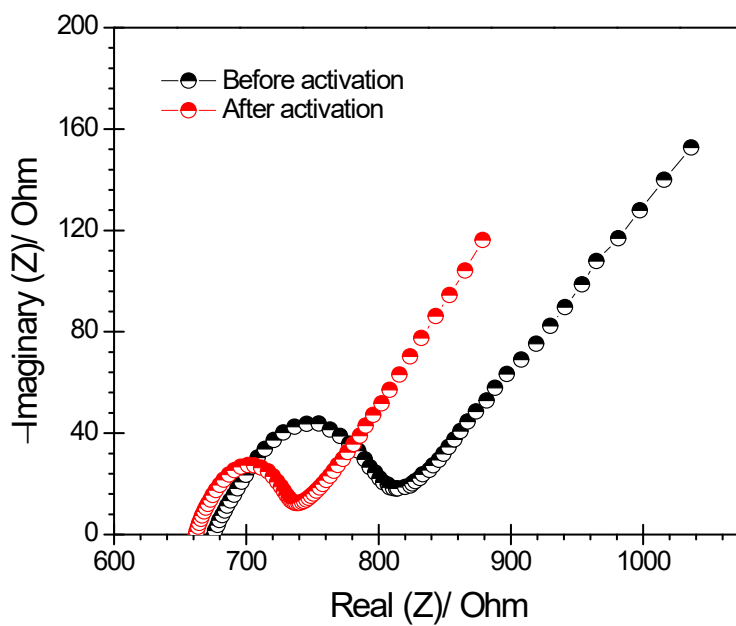


Figure S25. Nyquist plots of the supercapacitor before and after 60 CV cycles.

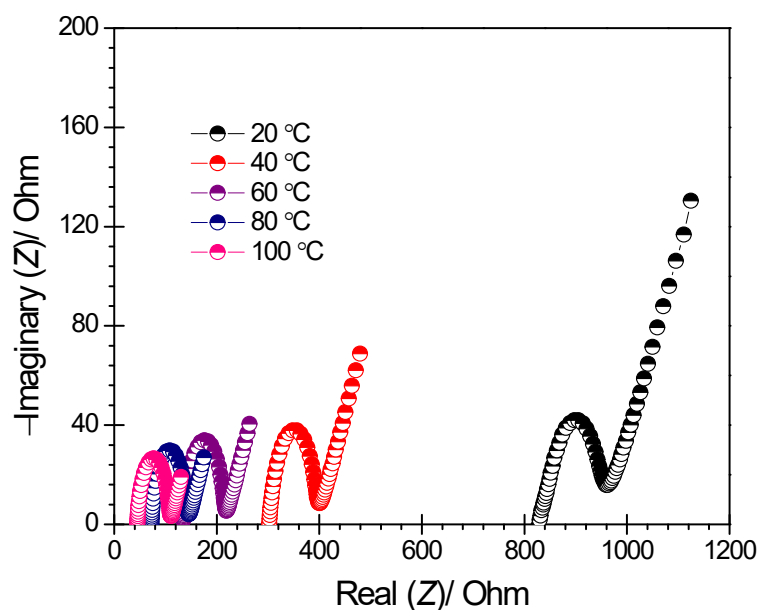


Figure S26. Different temperature EIS plots of the supercapacitor.

Table S1. Anodic and cathodic limits potentials and electrochemical stability windows (ESWs) on platinum working electrode at a scan rate of 0.001 V s^{-1} and at $20 \text{ }^\circ\text{C}$.

Ionic Liquid	E_C (V vs Fc/Fc ⁺)	E_A (V vs Fc/Fc ⁺)	ΔE (V)
[MmMIm][TEEP]	-1.10	3.47	4.57
[EmMIm][DEEP]	-1.11	3.25	4.36
[MmDMIm][TEEP]	-1.54	4.34	5.88
[EmDMIm][DEEP]	-2.33	2.93	5.26

Table S2. VFT equation parameters and apparent energies of activation for the ionic conductivity data.

Ionic Liquid	σ_0 (m ² /s)	B (K)	T_0 (K)	E_σ (kJ/mol)
[MmMIm][TEEP]	0.542	1227	153	10.2
[EmMIm][DEEP]	0.709	1279	156	10.6
[MmDMIm][TEEP]	0.725	1378	152	11.5
[EmDMIm][DEEP]	0.348	1176	164	9.78

Table S3. VFT equation parameters and apparent activation energy for the ion diffusivity data.

System	Ion	$D_0 \times 10^{-9}$ m ² /s	B, K	T_0 , K	E_D , kJ/(mol)
[MmMIm][TEEP]	anion	7.91	786	195	6.5
	cation	6.48	760	198	6.3
[EmMIm][DEEP]	anion	14.3	811	184	6.7
	cation	15.1	887	176	7.4
[MmDMIm][TEEP]	anion	19.6	1070	180	8.9
	cation	15.2	1013	184	8.4
[EmDMIm][DEEP]	anion	3.64	626	213	5.2
	cation	5.55	753	201	6.3

Table S4. Water content of the ILs

Ionic Liquid	Water Content (ppm)
[MmMIm][TEEP]	95 ± 5
[EmMIm][DEEP]	88 ± 5
[MmDMIm][TEEP]	97 ± 5
[EmDMIm][DEEP]	78 ± 5